# MAXIMUM LIKELIHOOD ESTIMATION OF YOUNG'S MODULUS IN TRANSIENT ELASTOGRAPHY WITH UNKNOWN LINE-OF-SIGHT ORIENTATION

*M. Charbit, E. D. Angelini*

{maurice.charbit, elsa.angelini}@telecom-paristech.fr
Institut Telecom, Telecom ParisTech, CNRS LTCI, Paris, FRANCE

*S. Audiere*

stephane.audiere@echosens.com
Echosens, Paris, FRANCE

## ABSTRACT

Transient elastography can be used to measure tissue elasticity by applying a mechanical stress constraint and measuring the velocity of propagation of the induced shear wave, assumed to be proportional to tissue elasticity. In this paper we study two original maximum-likelihood (ML) approaches for shear wave velocity estimation on RF ultrasound signals acquired with a transient elastography setup. For acquisitions made with a line of sight (LOS) aligned with the directions of propagation (DOP) of the shear wave, a simple parametric model was derived from the theoretical Green's function, enabling ML estimation of the elasticity. For non-aligned LOS and DOP, an empirical approach was considered to learn a simple time-delay model of the displacement field, using an annotated database of simulated data. A ML estimator was then defined to jointly estimate the angle of the LOS and the elasticity of the tissue. The proposed methods were evaluated on simulations, and RF signals acquired on phantom objects and on volunteers, for liver screening. Results reported very high accuracy, with elasticity errors of measures below $10\%$.

***Index Terms***— Ultrasound, transient elastography, tissue elasticity, shear wave, maximum likelihood estimator, Green's function, liver fibrosis.

## 1. INTRODUCTION

During the last decade, several shear-wave based elastography scanning approaches have been investigated for measuring mechanical properties of biological soft tissues. Elastography is particularly useful to assist practitioners to diagnose liver fibrosis based on the assumption that the pathological stage of the liver is directly related to its elasticity. Elasticity is defined by the Young's modulus $E$ and is related, under linear elastic assumptions, to the shear wave velocity $V_s$ inside the liver, through the relation $E \approx 3\rho V_s^2$ where $\rho$ denotes the mass density of the tissue [2]. Because most biological tissues are essentially composed of water, $\rho$ may be taken equal to 1. In transient elastography, shear waves are generated using a circular piston inserted in the center of a single-element ultrasound probe positioned on the surface of the skin. The piston is excited with a short pulse, typically designed as a single period of a sine wave, whose frequency ranges between 50 and 500 Hz. The shear wave velocity $V_s$ is estimated through the evaluation of point displacements within the liver. A common way to access the displacement field is to use ultrasonic scanning and measure correlations between successive RF lines observed along a fixed line of sight (LOS) using the single-element ultrasonic probe. Such approach assumes that the LOS coincides with the direction of propagation (DOP) of the shear-wave. This assumption can be altered significantly if the LOS direction is not perpendicular to the liver interface, due to diffraction phenomena. A recent study [1] has proposed a multi-correlation computation and shape analysis of depth correlation profiles to derive shear wave velocity values. The method claims to be independent of the direction of the LOS but the estimator is based on a shape factor difficult to predict and control in practice. In this work we propose an alternative approach, formulating a parametrical model of the displacements within the tissue and fitting this model with the observations using a maximum likelihood (ML) criterion.

In wave propagation problems, an explicit relation between the stress constraint applied to a medium and the generated displacement field within this medium can be derived with the Green's functions. Boundary conditions must be specified on the limits of the medium and the spatial extent of the constraint. In our experiments, we considered that the stress constraint is produced by a cylindrical piston acting normally on the planar surface of a semi-infinite medium. This setup corresponds to the one used in [3] to model the Fibroscan probe and motivated by the fact that the dimensions of the organ being screened are greater than the wavelength of the acoustic wave. An illustration of transient elastography scanning setup is provided in Figure 1. In the case where the DOP coincides with the LOS, the Green's function was derived in [3]. We show in this work that it can be used as a parametric model to estimate the shear wave velocity $V_s$ from displacement measures made on RF lines. In the case where the DOP does not coincide with the LOS, the Green's function seems to be intractable. As an alternative, we propose to formulate a simple model for the point-wise displacement field in the medium as a delay function that depends on the scanning setup parameters.

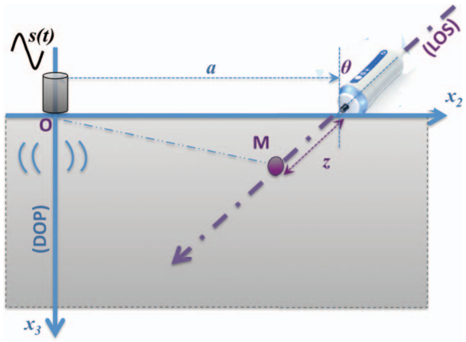


**Fig. 1**. *Setup of transient elastography scanning. Parameters include the direction of propagation (DOP) of the shear wave and the line of sight (LOS) used to record the RF lines. In the general case, the LOS can be shifted (by a) and tilted (by angle θ) with respect to the DOP.*

Using a simple delay model, we show that delay values can be learned on a database of RF lines using a parametrical regression approach. A ML criterion can then be used on new measures to jointly estimate the shear wave velocity and the direction of the LOS. Regarding the delay model itself, we show on simulated data that a simple spherical model is not valid but that a regression approach leads to an acceptable time-delay model. In particular, assuming that the depth-attenuation of the RF signals is also unknown, we were able to derive an algorithm that estimates both the shear wave velocity $V_s$ and the angle $\theta$ between the DOP and the LOS.

## 2. DISPLACEMENT FIELD FROM GREEN'S FUNCTION

The Green's function for the shear wave propagation in a semi-infinite medium stimulated by an impulse was derived in [3], for a setup illustrated in Figure 1. Using a Cartesian coordinate system $(x_1, x_2, x_3)$, a stress constraint $s(t)$ is applied by a cylindrical piston with radius $R$, along the normal of the planar surface $(x_1, x_2, x_3 = 0)$ of a semi-infinite medium. The piston is located at $x_1 = x_2 = x_3 = 0$. In [3] the probe is also located at the origin and the LOS coincides with the DOP (i.e. $\theta = 0$ and $a = 0$). The DOP corresponds to the line $x_3 > 0$ in the plane $x_2, x_3$. With this setup and parameterization, it can be shown that the displacement field within the medium has only one component $u_3(x_3, t)$ along the $x_3$-axis that writes:

$$u_3(x_3;t) \quad = \quad \frac{R^2}{\rho} \frac{1}{(x_3^2 + R^2)^{3/2}} \int_0^{\tau_s} \tau s(t-\tau) d\tau \quad (1)$$

where $\tau_s = \sqrt{x_3^2 + R^2}/V_s$. Using the expression (1), we can therefore compute analytically the response of a medium (characterized by its elasticity $E$ through $V_s$) to a given stress $s(t)$, as a displacement field $u_3$. We can measure displacements within the medium, via RF signal observations $y$ sampled on time intervals $T_s$ and spacing intervals $Z_s$. These measures are related to the displacement field within the medium via the following simple model:

$$y[m,n] = \beta[m]\, u_3[m,n;E] + w[m,n], \qquad (2)$$

where $(m,n) \in [1\ M] \times [1\ N]$, $u_3[m,n;E] = u_3(mZ_s, nT_s)$ and $\beta[m]$ is the unknown attenuation factor, which varies in depth. The noise term $w[m,n]$ encodes both the measurement noise and the discrepancy between the model used to compute the displacement of RF lines and the true displacement. We denote by $\mu = (\beta, E)$ the parameter of interest. Under Gaussian assumption, the maximum likelihood estimation is obtained with a least-square criterion that writes: $\hat{\mu} \quad = \quad \arg\min_\mu \sum_{m=1}^{M} \sum_{n=1}^{N} |y[m,n] - \beta\, u_3[m,n;E]|^2$. Minimization w.r.t. $\beta$ yields:

$$\hat{E} = \arg\max_E \frac{\left|\sum_{m,n} y[m,n] u_3[m,n;E]\right|^2}{\sum_{m,n} y^2[m,n] \sum_{m,n} u_3^2[m,n;E]} \qquad (3)$$

Computing a close-form expression of $\hat{E}$ is out of range but the maximization of Eq. 3 may be performed via exhaustive testing on a fine grid of values of $E$.

### 2.1. ML estimation of Young's modulus on displacement

#### FEM simulations

The elastography experiment was first simulated with a FEM solver[1] for a purely elastic medium and a simple geometry. In this work we studied a cylindrical geometry (90 mm high and 90 mm wide), and different elasticity values. The cylindrical piston of the experimental setup illustrated in Figure 1 was simulated with a diameter $R = 9$ mm and the LOS coincided with the DOP, normal to the planar interface.

The stress pulse was designed as a period of sinusoid at 150 Hz with apodization. We report in Figure 2, input and output components of the FEM simulation, and in particular the displacement field along a scan line, as a function of time. The ML criterion maximized in Equation (3)) is also plotted on elasticity grid values from 0 to 70 kPa by step of 0.2 kPa. The maximum was reached at $E = 12.0$ kPa while the true value used to generate the simulated displacement field was 12 kPa.

A series of comparison was performed between true and estimated elasticity values for different stress pulse frequencies (in the range [50 500] Hz) and different elasticity values (in the range [6 60] kPa). Relative errors are reported in Figure 3, which all remain below 10%. This first series of experiments confirms that maximization of the ML criterion is

[1] we used the FEM solver from the COMSOL Multiphysics software environment.

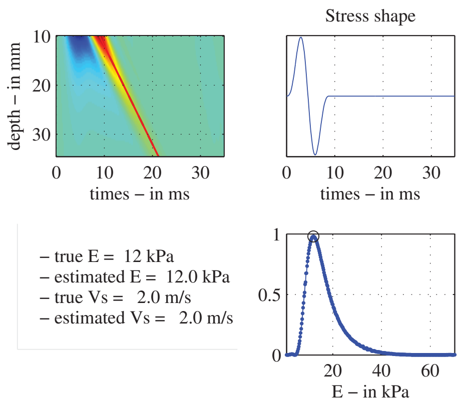


**Fig. 2**. *ML estimation of E on simulated data. (top left) Simulated displacement field. (top right) Stress temporal profile in arbitrary unit (A.U.) applied with a cylindric piston. (bottom right) Likelihood critrion in A.U. versus $E$.*

capable of estimating accurately the elasticity of a medium, exploiting an analytical expression of the displacement field and simulated measures (using a FEM solver).

### In-vivo experiments

We evaluated our proposed model on a phantom object (made with gelatin material) and on *in-vivo* data acquired on four volunteers. RF signals were recorded with the Fibroscan (Echosens, Paris) which was also used to provide a reference value of the elasticity of the medium. ML estimations of the $E$ values are reported in Table 1. This series of experiments shows very high agreements of measures, with errors below $10\%$, and average errors of $6\%$ for the phantom and $9\%$ for the volunteers.

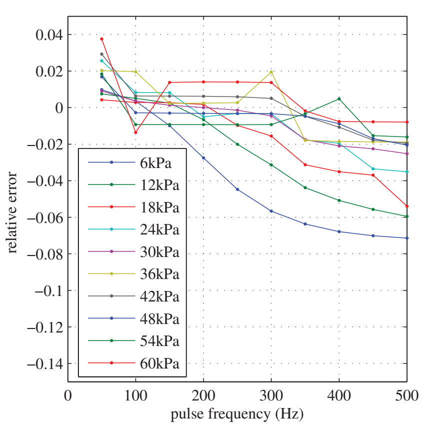


**Fig. 3**. *Relative errors of ML elasticity estimations versus stress frequency using FEM simultations with different $E$ values.*

| | $E$ (ML) | $E$ (FibroScan) |
|---|---|---|
| Phantom | $E = 31.18$ kPa, | $E = 34.00$ kPa |
| Phantom | $E = 27.36$ kPa, | $E = 27.00$ kPa |
| Phantom | $E = 6.66$ kPa, | $E = 6.10$ kPa |
| Volunteer | $E = 8.7$ kPa | $E = 8.67$ kPa |
| Volunteer | $E = 4.35$ kPa | $E = 5.00$ kPa |
| Volunteer | $E = 3.48$ kPa | $E = 4.10$ kPa |
| Volunteer | $E = 23.92$ kPa | $E = 23.90$ kPa |

**Table 1**. *In-vivo tissue elasticity estimations: $E$ values from ML estimations on RF measures and from the Fibroscan are reported for 2 series of experiments on gelatin phantom objects and on volunteers.*

## 3. EMPIRICAL TIME-DELAY MODEL FOR DISPLACEMENT FIELDS

### 3.1. Empirical time-delay model

When the DOP does not coincide with the LOS, we do not have an analytical expression of the Green's function to compute the displacement field. To circumvent this difficulty, we propose to construct an empirical model of the displacement field, based on numerical measures. We consider that the source signal can be viewed as a point, located at the center of the piston. As illustrated in Figure 1, we call $z$ the linear abscissa of the RF measures acquired along the LOS, $a$ the distance between the LOS and the center of the piston and $\theta$ the angle between the LOS and the DOP. The piston located at point $O$ acts normally to the planar interface $(x_1, x_2)$ where $x_1$ is orthogonal to the plane $(x_2, x_3)$.

In this configuration, observation are made at positions: $x_2 = a + z\sin(\theta)$, $\quad x_3 = z\cos(\theta)$. We propose to express the displacement field $u(z;t)$ based on the following time-delay model along the LOS:

$$u(z + \Delta z; t) = \beta(z) u(z; t - \Delta t)$$

where $z$ is the linear abscissa along the LOS, and:

$$\Delta t = \tilde{\tau}(z; E, \theta) + T_0 \tag{4}$$

For example, in the case of a spherical wave propagation[2], the delay can be written as:

$$\begin{aligned} \tilde{\tau}(z; E, \theta) &= \frac{d(z;\theta)}{\sqrt{E/3}}, with \\ d(z;\theta) &= \sqrt{a^2 + z^2 - 2az\sin(\theta)} \end{aligned} \tag{5}$$

We used FEM simulations, as previously described, with a stress frequency $s(t)$ of 100 Hz and a distance between the LOS and the DOP set to $a = 20$mm. We then analyzed the relation between the delay measured by maximum of correlation on the simulated trajectories and the spherical delay

[2]Note that, for plane waves, the parameter $\theta$ is not identifiable.

modeled in Equation (6). Comparison was performed for a set of $E$ values from 6 kPa to 60 kPa, with 6 kPa increments. For each $E$ value, we varied $\theta$ from $-30°$ to $30°$ by steps of $5°$. We observed that no ($E$,$\theta$) pairs lead to a validation of the spherical model given by Equation (6). This initial observation highlights the need for empirical learning of the time dependency of the delay with respect to the parameters $z$, $E$ and $\theta$. We propose to learn the following empirical delay model:

$$\tilde{\tau}(z; E, \theta) = \alpha_0(E, \theta) + \alpha_1(E, \theta)d + \alpha_2(E, \theta)d^2 \qquad (6)$$

where $d(z; \theta)$ is defined in Equation (5). The regression parameters $\alpha_i, i = 0, 1, 2$ were learnt as a double-entry array depending on ($E$, $\theta$), on a database of FEM-based simulated data.

### 3.2. Model of RF-based displacement measures

Working with the time-delay model defined in Equation (6) and learned on simulated data, we can derive a model for the RF-based displacement measures within the tissue, as:

$$y(z, t + \tilde{\tau}) \quad = \quad \beta(z)\, u_s(t) + b(z, t) \qquad (7)$$

where $u_s(t)$ denotes the generic shear-wave displacement front, $\beta(z)$ is an unknown attenuation term depending on $z$, and $b(z, t)$ is the measurement noise assumed to be centered Gaussian with unknown variance $\sigma^2$. The signal $u_s(t)$ is also assumed to be Gaussian, centered, with unknown variance $\sigma_s^2$. Measures are acquired on time intervals $T_s$ and spatial intervals $Z_s$. We let $u[m, n; \theta, V_s] = u(mZ_s, nT_s + \tau_m(\theta, V_s))$, $u_s[n] = u_s(nT_s)$ and $b[m, n] = b(mZ_s, nT_s)$ and write:

$$y[m, n; \theta, V_s] = \beta[m]u_s[n] + b[m, n] \qquad (8)$$

For $m \in [1 \cdots M]$, concatenating the $M$ observations as a vector, we may write in vector forms:

$$\mathbf{y}[n; \theta, V_s] = \boldsymbol{\beta} u_s[n] + \mathbf{b}[n] \qquad (9)$$

Under Gaussian assumption, the likelihood function can be derived and its maximization w.r.t. $\beta$, $\sigma$ and $s$ has a close form expression, that is based on the eigenvectors of the empirical covariance matrix of the delayed signals. Maximization w.r.t. $\theta$ and $V_s$ has to be performed numerically, via exhaustive search. Shannon's interpolation was used on non-integer delay values.

### 3.3. Experiments on joint estimations of ($E$,$\theta$)

A set of FEM simulated data was generated with the following parameters: stress frequency of 100 Hz, LOS shift $a = 20$mm, $\theta$ in $[-30° \;\; +30°]$ with increment steps of $5°$ and $E$ in the range $[6 \;\; 60]$ kPa with increment steps of 6 kPa. In total 130 files were generated with the FEM solver: 102 files were used for learning the regression coefficients of the linear model in Equation (6), and 28 files were used to test the joint ML estimator of $E$ and $\theta$. Pairs of values ($E$, $\theta$) to estimate in the test database were not represented in the learning database. Results, reported in Figure 4, reported a relative error smaller than 5% for the Young's modulus.

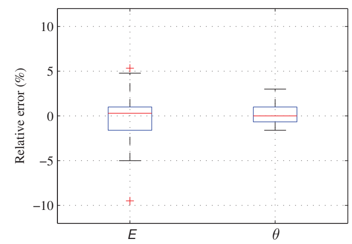


**Fig. 4**. *Box and whiskers plots of the relative errors for $E$ and $\theta$ estimations, on FEM simulated data*

## 4. CONCLUSION

In this work, we proposed a parametrical statistical model and a maximum likelihood estimation of Young's modulus $E$ for transient elastography screening setup. Two configurations of interest were studied to derive models of displacement fields within a tissue: (1) when the LOS and DOP coincide ($\theta = 0$), we proposed a model derived from the Green's function, (2) when the LOS and DOP are not aligned ($\theta \neq 0$), we proposed an empirical time-delay model learned on a database of observed motion fields for varying experimental conditions w.r.t. ($E$, $\theta$). For the first case, numerical results on simulations and *in-vivo* RF data acquired showed very high agreement with reference values. The second approach was evaluated on simulated data, where the LOS direction was perfectly controlled. Results demonstrated the capability to perform elastography measures without the need to align the LOS and the DOP, and opens a path to new elastographys scanning setups.

## 5. REFERENCES


[1] N. Benech, S. Catheline, J. Brum, T. Gallot, and C. A. Negreira, 1-D Elasticity Assessment in Soft Solids from Shear Wave Correlation: The Time-Reversal Approach, *IEEE Trans. on UFFC*, vol. 56, no. 11, November 2009.

[2] L. Sandrin, M. Tanter, J.L. Gennisson, S. Catheline, and M. Fink, Shear Elasticity Probe for Soft Tissues with 1-D Transient Elastography, *IEEE Tr. on UFFC*, vol. 49, no. 4, April 2002.

[3] L. Sandrin and D. Cassereau and M. Fink, The role of the coupling term in transient elastography, *J. Acoust. Soc. Am., vol. 115, N. 1*, Jan. 2004, pp 73-83.

[4] A. Lhemery, A model for the transient ultrasonic fields radiated by an arbitrary loading in a solid, *J. Acoust. Soc. Am., vol. 96, N. 1*, 1994, pp 3776-3786.

[5] K. Aki and P.G. Richards, *Quantitative Seismology: Theory and Methods*, Freeman, San Francisco, 1980, Vol. 1, Chap. 4, p. 74.